

Review

Studies of chromium cages and wheels

Eric J.L. McInnes^a, Stergios Piligkos^a, Grigore A. Timco^{a,b}, Richard E.P. Winpenny^{a,*}

^a Department of Chemistry, The University of Manchester, Oxford Road, Manchester M13 9PL, UK

^b Institute of Chemistry, Moldova Academy of Sciences, Chisinau, Republic of Moldova

Received 15 October 2004; accepted 6 February 2005

Available online 26 April 2005

Contents

1. Introduction	2577
2. Dodecanuclear chromium cages and related clusters	2578
2.1. $[\text{Cr}_{12}\text{O}_9(\text{OH})_3(\text{O}_2\text{CCMe}_3)_{15}]$ 1	2578
2.2. Magnetic properties	2578
2.3. EPR spectroscopy	2579
2.4. Optical spectroscopy	2580
2.5. Synthesis of related compounds and hybrid materials	2581
3. Octanuclear chromium and heterometallic wheels	2581
3.1. $[\text{Cr}_8\text{F}_8(\text{O}_2\text{CCMe}_3)_{16}]$ 4	2581
3.2. $[\text{NH}_2\text{R}_2][\text{Cr}_7\text{MF}_8(\text{O}_2\text{CCMe}_3)_{16}] \{\text{Cr}_7\text{M}\}$	2583
3.3. Possible applications of $\{\text{Cr}_7\text{M}\}$	2584
3.4. Wheels containing non-octahedral metal divalent metal ions	2585
3.5. Chromium horseshoes	2586
3.6. Other templates	2586
3.7. Some thoughts on how the heterometallic wheels form	2588
Acknowledgments	2589
References	2589

Abstract

Studies of two distinct classes of chromium(III) cage complexes are discussed. The first are compact oxo- and carboxylate cages, made by heating precursors to high temperature under a flow of nitrogen. One of these cages, $[\text{Cr}_{12}\text{O}_9(\text{OH})_3(\text{O}_2\text{CCMe}_3)_{15}]$, has an $S=6$ spin ground state which proves a very interesting subject for study by EPR and MCD spectroscopy. Use of other carboxylates leads to other octa- and dodeca-nuclear complexes. The second class of compounds are homo- and hetero-metallic wheels and chains bridged by fluoride and carboxylates. These include the first heterometallic anti-ferromagnetically coupled ring systems and are being widely studied in areas as diverse as magnetic cooling and quantum information processing. The mechanism by which these unusual cyclic and acyclic structures form is discussed.

© 2005 Elsevier B.V. All rights reserved.

Keywords: Chromium cages; Synthetic methods; Structure formation; Magnetism

1. Introduction

The study of paramagnetic metal cages or clusters took off in the late 80s and early 90s. In the West, this was largely

* Corresponding author. Tel.: +44 16 1275 4653; fax: +44 16 1275 4616.
E-mail address: richard.winpenny@man.ac.uk (R.E.P. Winpenny).

due to a few very influential groups, e.g. Lippard's work on iron(III) clusters [1], or Christou's work on manganese cages [2], or the Gatteschi group's investigations of the magnetic properties of a variety of compounds [3]. New results were reported regularly for all the common paramagnetic 3d metal ions, with one noticeable exception: chromium(III) was largely ignored. This absence may have been caused for a variety of reasons: since there is no significant metalloenzyme that contains a polymetallic chromium site, the biological significance of this class of compounds is negligible, although recently some medical applications have been considered, e.g. [4]. Moreover, probably there was a subconscious feeling that all polynuclear chromium(III) complexes were likely to be oxo-centred carboxylate triangles [5]. To complete the picture, the high crystal field stabilisation energy of chromium(III) determines a well-known pronounced lack of reactivity that made its synthetic chemistry quite difficult.

However, this Western opinion did not appear to be shared in Moldova. In the early 1990s, two new clusters were reported [6,7], derivatives of which we have now studied very heavily, and which have opened up two different approaches to doing polymetallic chemistry. The physics of the new compounds is interesting, and the synthetic methods used to prepare both suggest new paths to be explored.

The two compounds are made in different ways, but both ways use conditions that appear rather extreme to a conventional coordination chemist. Both were made as part of a study of the use of chromium compounds in catalysis of oxidation and polymerisation reactions. The interest in their magnetic properties dates from the late 90s, when we began to look at their properties in collaboration with many international partners.

2. Dodecanuclear chromium cages and related clusters

2.1. $[Cr_{12}O_9(OH)_3(O_2CCMe_3)_{15}]$ **1**

Compound **1** shows a compact structure containing 12 chromium(III) ions arranged as a centred pentacapped trigonal prism (Fig. 1). The first full report on this cage describes its synthesis precisely [6], but it is not a synthesis that most coordination chemists would recognise. Chromium nitrate is mixed with sodium pivalate in hot water, causing an immediate blue precipitate. This precipitate is collected and heated to 400 °C under a stream of dry nitrogen. The dark green solid that is formed contains **1** but it has to be recrystallised from *n*-propanol to purify it, and to make crystals suitable for X-ray analysis.

The original paper made a mistake in the formula, reporting it as $[Cr_{12}O_{12}(O_2CCMe_3)_{15}]$. This attracted our attention because it implies mixed valent Cr(III)/Cr(IV); mixed valency often leads to fascinating magnetic proper-

ties. However, repeating the work we crystallised a form which had D_3 crystallographic symmetry [8], and it was clear that all the metal sites are Cr(III), and that charge balance must be achieved in some other way. The structure contains six μ_4 -oxygen sites and six μ_3 -oxygen sites. When a neutron structure [8] was performed, it was clear there was a half-occupancy hydrogen attached to each μ_3 -oxygen, hence, the formula is $[Cr_{12}(\mu_4-O)_6(\mu_3-O)_3(\mu_3-OH)_3(O_2CCMe_3)_{15}]$.

2.2. Magnetic properties

The ground state of the molecule is $S = 6$ but the spin state structure is clearly unusual [8]. This is best seen from looking at a plot of $\chi_m T$ against T (Fig. 2), where there is a double maximum. This suggests that the highest energy states have very low spin ($S = 0, 1$, etc. ...) and these are depopulated first as temperature falls. After passing through a maximum the value of $\chi_m T$ falls—suggesting that the highest spin states ($S = 18$, etc. ...) are being depopulated. There is a final rise at low T , which is due to exclusive population of the $S = 6$ ground state. This unusual profile has proven very useful, as we can use it as fingerprint for proving the structure of **1** is retained in unusual situations, for example when incorporated in a microporous supports (see below). The ground state is proven by magnetisation measurements and EPR spectroscopy, but the complexity of the structure makes it impossible to fit the variable temperature susceptibility behaviour to derive exchange interactions.

Low temperature magnetic studies of single crystals of **1** show hysteresis in magnetisation against field measurements [9] (Fig. 3), but this hysteresis is due to non-equilibrium behaviour—a “phonon bottleneck” in physics-speak and not due to an energy barrier. The ground state of $S = 6$ contains $2S + 1$ microstates defined by the quantum number M_s which takes the values from $+S$ to $-S$ in integer steps. These M_s states are not degenerate, but they are split in zero-field with the energy gaps between levels being related to a parameter D , called the axial zero-field splitting. For **1**, D is positive, and this makes the ground state $S = 6$, $M_s = 0$. This contrasts to the single molecule magnets where D is negative and the ground state is always degenerate in zero-field and given by $M_s = \pm S$.

The hysteresis that is seen for **1** arises (Fig. 3) because as the field is increased, the ground state changes at regular intervals as the $M_s = 1, 2, 3, 4, 5$ and 6 states fall in energy because they are stabilised by interaction with the magnetic field. Therefore, at the highest field measured the ground state, $|S, M_s\rangle$, becomes $|6, -6\rangle$. When the field is swept in the reverse direction there is insufficient thermal energy in the system—too few phonons—to allow transitions to the other $|6, -M_s\rangle$ states, which are now lower in energy than the $|6, -6\rangle$ state. Therefore, the loss of magnetisation of the sample does not quite keep up with the lowering of the field, and the return plot does not follow the upper curve. This gives an apparent hysteresis.

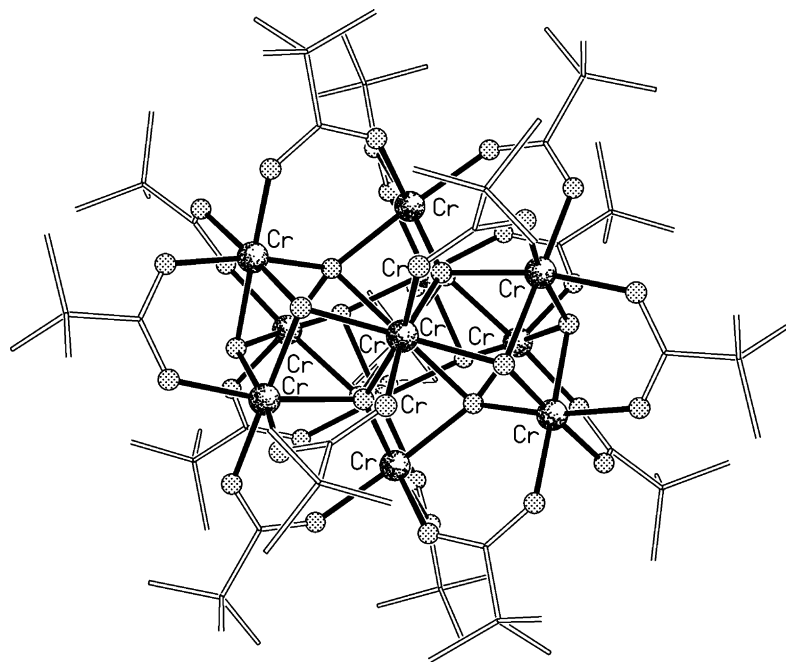


Fig. 1. The structure of $[\text{Cr}_{12}\text{O}_9(\text{OH})_3(\text{O}_2\text{CCMe}_3)_{15}] \mathbf{1}$ in the crystal. (Shading for all structural figures: Cr, heavy random pattern; O, regular spots; N, diagonal stripes; F, shaded with highlight; other metals, cross-hatched; C, drawn as lines; H, omitted for clarity. Based on data in [8].)

While the phenomenon is not as interesting as “single molecule magnetism”, we can use this hysteresis to measure the D -value as $+0.08 \text{ cm}^{-1}$ [9]. As the ground state changes by steps in M_s then the magnetisation should also change—producing a “staircase” (Fig. 3b). This is similar to the steps reported for $[\text{Fe}(\text{OMe})_2(\text{O}_2\text{CCH}_2\text{Cl})]_{10}$, but there the steps are due to integer changes in S not M_s . The result is that for $\mathbf{1}$ the step functions are difficult to see but are much clearer from a plot of the first derivative. We can then use the spacing between the peaks to measure D directly.

2.3. EPR spectroscopy

While this is one method of deriving D , a better one is EPR spectroscopy, and $\mathbf{1}$ has proven a wonderful subject for EPR [8–10]. D is around 0.088 cm^{-1} , therefore, even at X-

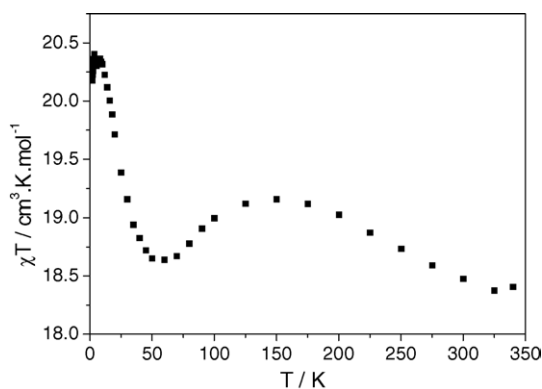


Fig. 2. $\chi_m T$ against T for $\mathbf{1}$.

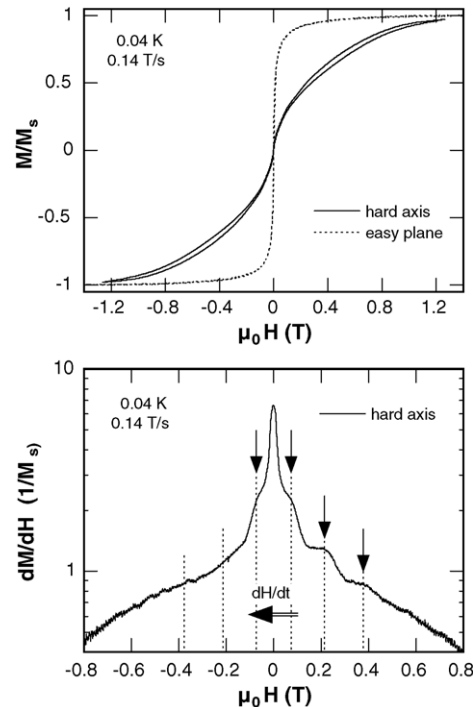


Fig. 3. (a) Plot of magnetization vs. magnetic field for $\mathbf{1}$ measured on a micro-SQUID with the magnetic field applied parallel (hard axis) and perpendicular (easy plane) to the molecular C_3 axis at 0.04 K and magnetic field sweep rate of 0.14 T s^{-1} . (b) Derivative of the curve in (a) corresponding to the hard axis for the field sweep from 1.4 to -1.4 T (Reproduced from [9] with permission.)

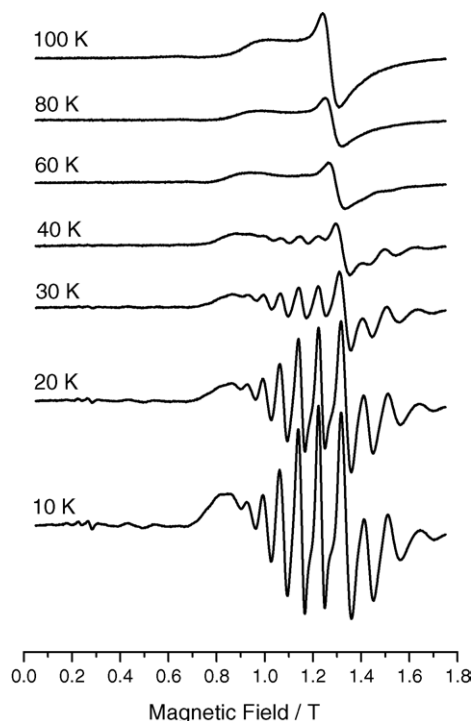


Fig. 4. Variable temperature Q-band EPR spectra of **1** recorded on a powder.

band, a multi-line spectrum is observed, which becomes very well resolved at K- and Q-band (Fig. 4). Fitting the EPR spectra has allowed us to find D precisely, but we can do much more because of the high symmetry of the cage (which makes requires that E is zero) and the coincidental fact that the zero-field splitting is close to the energy used in most EPR spectrometers.

For example, if we use high frequency radiation—180 GHz and higher—we can examine depopulation effects within the ground state spin manifold [9]. As peaks are seen due to transitions of $\Delta M_s = \pm 1$, we see 12 transitions within the $S = 6$ ground state if the thermal energy is sufficient that all M_s levels are significantly populated. However, as the temperature is lowered, we lose population in the higher M_s levels, and hence, intensity for some of the peaks within the ground state spin manifold. The peaks that lose intensity give a direct measure of the sign of D ; positive D will lead to different depopulation effects than negative D . Here, the study proves that D is positive, and **1** is not a single molecule magnet.

The availability of large single crystals and the high site symmetry of the molecule make the compound ideal for single crystal EPR spectroscopy. This has allowed us to match the molecular symmetry axes with the axes of the g- and D-tensors. As expected, the principle axes are coincident with the crystallographic three-fold axis passing through the molecule. In many ways, this simply confirms what we expected. However, we can take this further because the magnitude of D is such that we can do studies at X-band, and this opens the possibility of doing parallel mode EPR spectroscopy [10] as well as perpendicular mode.

Most people are unaware that there are two distinct experiments. A conventional EPR experiment with the magnetic field created by the microwave radiation is *perpendicular* to the external field. This creates the well-known selection rule that transitions are only seen when M_s varies by ± 1 . When the magnetic field created by the microwave radiation is *parallel* to the external field the selection rule is quite different and transitions are only seen between levels where the wavefunction contains contributions from the same M_s state: the selection rule is sometimes trivially written as $\Delta M_s = 0$. Our interest stemmed from an highly cited paper by Leuenberger and Loss [11], where they described a method for quantum computing involving writing information to an SMM using a mixture of perpendicular and parallel mode pulses. As we were unaware of any parallel mode studies of high spin molecules **1** offered an opportunity to test the feasibility of what Leuenberger and Loss had proposed.

The experiment—performed on aligned single crystals—conforms to theory [10]. When the external field is aligned parallel to the molecular Z-axis each energy level is described accurately by quantum numbers M_s , i.e. $M_s = 0$ is distinct from $M_s = 1$ or 2 or 3, etc. . . . Therefore, the wavefunctions for each energy level have only one M_s state contributing and the parallel mode spectrum contains no features. As we change the relative orientation of the field with respect to the molecular Z-axis, we mix the M_s levels and each energy level is now accurately described by wavefunctions containing contributions from several M_s levels. The result is that parallel mode transitions become allowed, with the transition probability dependent on the orientation of the molecule with respect to field as this controls the character of the individual energy levels. Comparing the result with the theory proposed by Leuenberger and Loss [11], we can say that parallel mode transitions can be seen in very high spin molecules, but that it is dubious whether the transition probabilities for multi-photon excitations (as required) would be sufficiently high to allow significant population of several energy states.

2.4. Optical spectroscopy

1 has an UV–vis spectrum at room temperature that resembles that of monomeric Cr(III), with two d–d absorptions at 16 475 and 22 883 cm^{-1} [12]. The MCD spectrum at 1.8 K has much greater resolution, for example resolving the former band into two transitions, assigned to the ${}^4A_2 \rightarrow {}^4A_1$ and ${}^4A_2 \rightarrow {}^4E$ —which is consistent with the D_3 symmetry of the molecule (Fig. 5). Several sharper features are also observed in the MCD that can be assigned to spin-forbidden transitions—using assignments previously used for other Cr(III)O₆ chromophores [13–15].

Macfarlane has given analytical expressions for the ground state ZFS for trigonally distorted Cr(III) ions in terms of the energy gaps to the excited spin quartet and spin doublet states [16]. Using these expressions, we can calculate the single ion ZFS in **1** directly from the MCD spectra. Although there

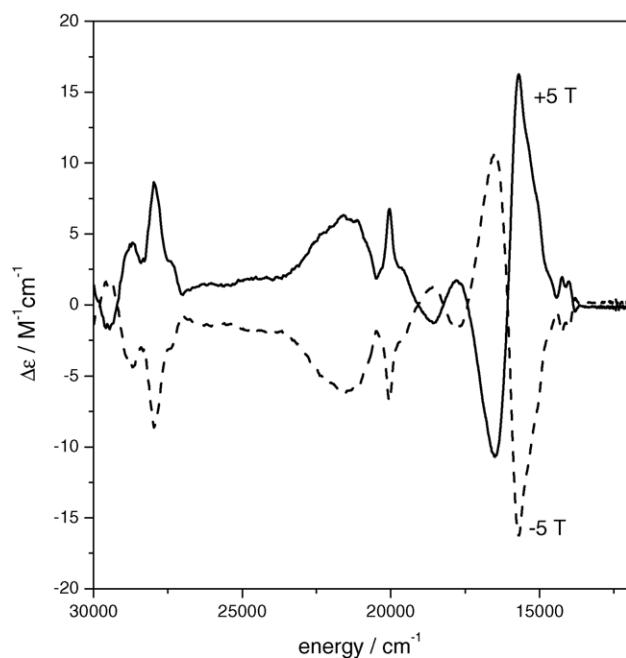


Fig. 5. MCD spectrum of **1** recorded on a frozen solution at 4 K.

are four crystallographically independent Cr(III) sites in **1**, their structural parameters do not vary significantly and the differences are not resolved in the optical spectra. We are, therefore, calculating a mean single ion ZFS from the optical data.

We calculate a $|D| = 1.035 \text{ cm}^{-1}$ for the single ion. We can then use the vector coupling approach [17] to relate the single ion ZFS to the measured ZFS for the $S = 6$ state of the cluster. To do this a coupling scheme needs to be defined that leads to an $S = 6$ state from 12 $S = 3/2$ ions arrayed on the vertices of a centred-pentacapped-trigonal prism. Two rational schemes can be proposed [9], which give $D_{S=6} = \pm 0.091$ or $\pm 0.142 \text{ cm}^{-1}$. EPR has told us the sign and magnitude of $D_{S=6}$ and the former coupling scheme is in remarkable agreement. The conclusion is that the ZFS in **1** is almost entirely due to single ion contributions from Cr(III) ions. However, a disturbing aspect of the calculation is that the frequently used vector coupling approach [17] is extremely dependent on the coupling scheme adopted. It is very easy to choose arbitrary coupling schemes, and the justification for the specific one chosen is often unclear.

2.5. Synthesis of related compounds and hybrid materials

The high temperature approach to synthesis of **1** suggested many further experiments. For example, replacement of pivalate as the carboxylate in the synthesis leads to other new chromium cages.

If benzoate is used an octanuclear cage is formed: $[\text{Cr}_8(\mu_4\text{-O})_4(\text{O}_2\text{CPh})_{16}]$ **2**. This cage contains a $\{\text{Cr}_4\text{O}_4\}$ cubane core, capped by a further Cr centre on each oxide [18]. The overall structure, therefore, has non-crystallographic T_D symmetry

(Fig. 6). The symmetry still requires four exchange interactions to model the unique exchange paths. A method to model this data was developed by Luban et al. [19], based on a high temperature expansion of the weak-field susceptibility. This has advantages over more traditional means of fitting magnetic data—especially where multiple exchange interactions are present—as it removes the need to repeatedly diagonalize the Hamiltonian for different choices of the four independent exchange constants, which is extremely time-consuming. The results give two antiferromagnetic ($J/k_B = -4.8$ and -13.5 K) and two ferromagnetic exchange interactions ($J/k_B = 13.0$ and 24.0 K), and model the observed data well.

Changing to *iso*-butyrate or *tert*-butylacetate as the carboxylate leads to two related cages: $[\text{Cr}_{12}\text{O}_8(\text{O}_2\text{CR})_{20}(\text{H}_2\text{O})_4]$ **3** [20]. The structures of these cages are related to **2**, as they also contain $\{\text{Cr}_4\text{O}_4\}$ cubane cores (Fig. 7). However, here there are three face-sharing cubanes giving a central $\{\text{Cr}_8\text{O}_8\}$ tricubane. The external oxides are again each capped by a further Cr centre. The reason for the variation between structures is not entirely clear. We have proposed that it can be related to the pK of the carboxylic acid formed if the carboxylate present is protonated. However, we have not been able to prove this supposition. Eshel and Bino have used the same approach to make a similar dodecanuclear chromium cluster using propionate as the ligand [21].

The high stability of Cr(III) imposes the requirement to use high temperatures in making **1–3**, and this stability can be useful. **1** is a remarkably stable molecule—dissolving intact in concentrated acid for example. The spectroscopic and magnetic traces of the molecule are also very distinctive. The combination of properties makes it an excellent molecule for studying the preparation of hybrid materials containing high spin clusters incorporated in zeolitic hosts. We have reported some preliminary work in this field [22]. The results show that incorporation of clusters into mesoporous supports is possible, and dependent on the comparative size of the clusters and the pores within the zeolite. Thus, for small pore phases (ca. 25 \AA diameter), the clusters are not incorporated within the structure. For larger pores, **1** is incorporated more easily than **3**, which involve larger carboxylates, and therefore, occupy greater volume. The Q-band EPR spectrum of **1** incorporated in the zeolitic hosts proves beyond doubt that the cage is intact [22].

3. Octanuclear chromium and heterometallic wheels

3.1. $[\text{Cr}_8\text{F}_8(\text{O}_2\text{CCMe}_3)_{16}]$ **4**

The second group of compounds arise from a slightly less unusual reaction. If hydrated chromium fluoride is reacted with hot pivalic acid in DMF a green material can be made which contains an octanuclear metal ring— $[\text{Cr}_8\text{F}_8(\text{O}_2\text{CCMe}_3)_{16}]$ **4** (Fig. 8). The compound was made in 1985, and the unusual structure led to a patent within

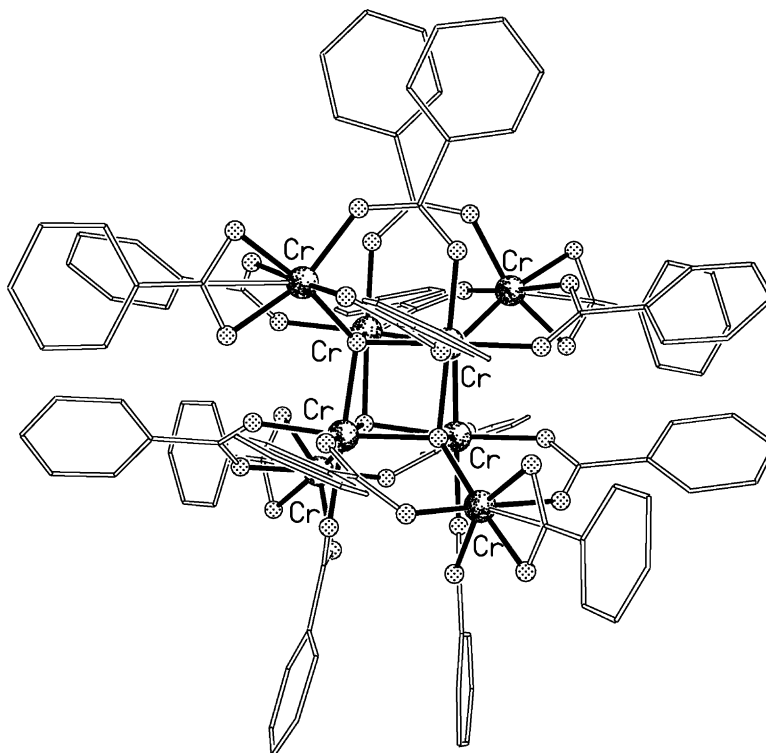


Fig. 6. The structure of $[\text{Cr}_8(\mu_4\text{-O})_4(\text{O}_2\text{CPh})_{16}]$ **2** in the crystal. (Based on data in [18].)

the former Soviet Union [23]. This delayed publication of the structure until 1991 [7]; it was discovery of a form which crystallises in a tetragonal space group that began interest in the magnetic properties of the family [24].

The wheel is anti-ferromagnetically coupled, leading to an $S=0$ ground state. This makes it similar to the famous decanuclear “ferric wheel”, first reported by Lippard and co-workers [25]. We were, therefore, interested in examining the detailed magnetic properties of the compound. One set of experiments

involve torque magnetometry. This technique requires all the molecules in the crystal to be co-planar; hence, the importance of the tetragonal crystal symmetry. Torque measurements allow us to look at the transition from the $S=0$ ground state to the $S=1$ state, and allows us to calculate the zero-field splitting parameter, D , for this state as 1.6 cm^{-1} [24].

4 can be made in moderate yield from starting materials that can be deuterated; this allows us to pursue inelastic neutron scattering studies (INS) to derive spin Hamiltonian pa-

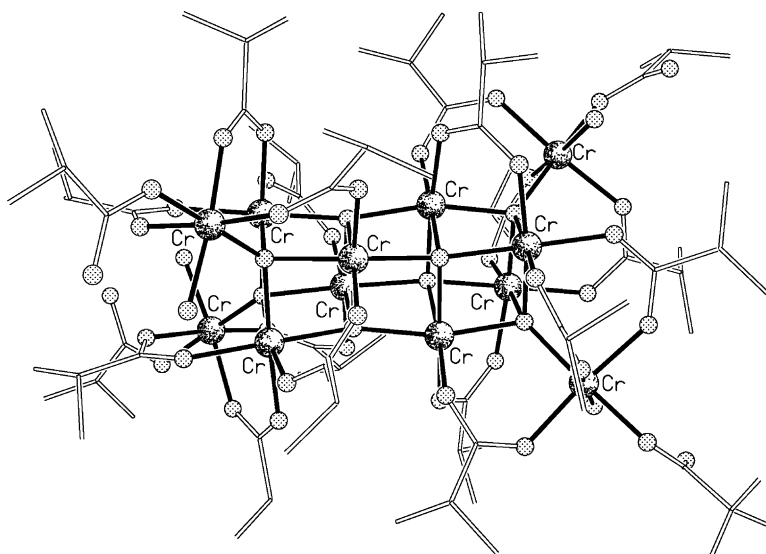


Fig. 7. The structure of $[\text{Cr}_{12}\text{O}_8(\text{O}_2\text{CHMe})_{20}(\text{H}_2\text{O})_4]$ **3** in the crystal. (Based on data in [20].)

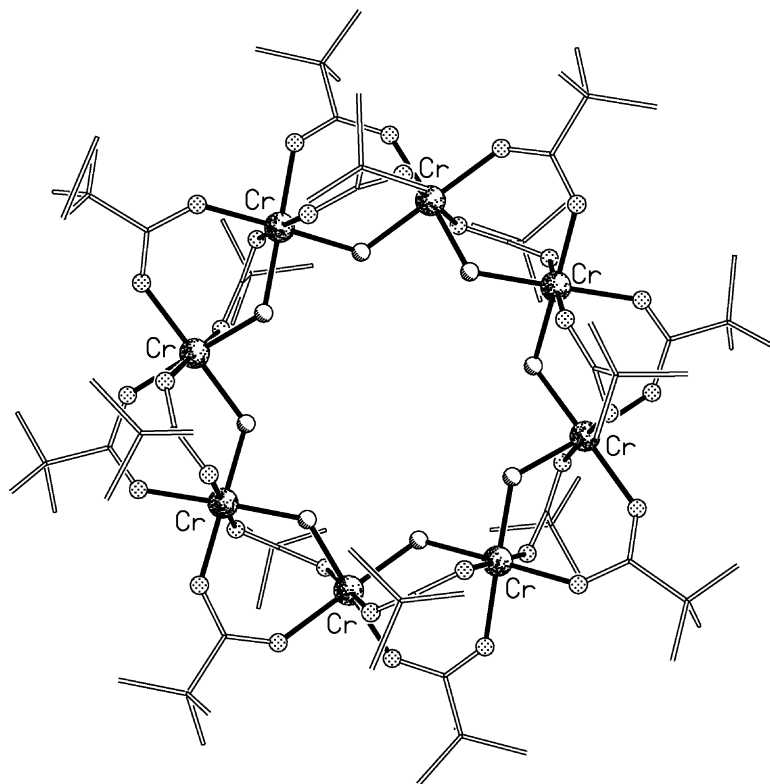


Fig. 8. The structure of $[\text{Cr}_8\text{F}_8(\text{O}_2\text{CCMe}_3)_{16}]$ **4** in the crystal. (Based on data in [7].)

rameters in detail, such as the exchange constant and to confirm D [26]. INS has the selection rules $\Delta S = 0$ or ± 1 , $\Delta M = 0$ or ± 1 . Therefore, at low temperature, the transitions are from the ground state, $|S=0, M=0\rangle$ to $|S=1, M=0\rangle$ and $|S=1, M=\pm 1\rangle$; two peaks should be seen, with their positions dependent on J and with the gap between the two peaks directly related to D . This gives a value of 0.21 meV (1.7 cm^{-1}), confirming results from high frequency EPR spectroscopy [21]. As the temperature increases, the $S=1$ state becomes thermally populated, and therefore, transitions are seen to the $S=2$ spin manifold. The J -value found by INS is 1.46 meV (11.8 cm^{-1}), which is identical to that obtained from fitting the variable temperature magnetic susceptibility. The data obtained has been further interpreted by Waldmann et al. [27] in terms of spin wave excitations; such an interpretation is beyond the understanding of simple chemists, but a good introduction is given elsewhere in this issue of Coordination Chemistry Reviews [28].

3.2. $[\text{NH}_2\text{R}_2][\text{Cr}_7\text{MF}_8(\text{O}_2\text{CCMe}_3)_{16}] \{\text{Cr}_7\text{M}\}$

4 offers an opportunity to perform detailed studies on an anti-ferromagnetic ring with an $S=0$ ground state. In some ways, it is a better subject for study than the original member of the family $\{\text{Fe}_{10}\}$. However, the synthesis can be modified to create a new class of magnetic molecule, a class that seems to contain an enormous potential for extension, producing several unprecedented structures.

We became interested in theoretical papers coming from the Loss group in Basel concerning the possible behaviour of antiferromagnetically coupled rings with non-zero ground states [29–31]. At this point, there were no pure compounds that existed that could be used to test these theories. The vast majority of cyclic complexes were even-numbered, and all were homometallic [32]. This combination means that the ground state for all these compounds is inevitably $S=0$.

If a single Cr(III) ion could be replaced with an ion with a different spin, then the ring would necessarily have a paramagnetic ground state. The best way to do this is to choose a divalent metal ion which will adopt the same coordination geometry as Cr(III) in **4**; if a source of this divalent metal ion is added to the reaction mixture you will make **4**—which is neutral—but also $[\text{Cr}_7\text{MF}_8(\text{O}_2\text{CCMe}_3)_{16}]$ which will be a monoanion. It should, therefore, be possible—if a cation is added to create an ion pair with $\{\text{Cr}_7\text{M}\}$ —to separate the neutral homometallic wheel from the monoanionic heterometallic ring. The charge-balancing cation we chose was a secondary ammonium cation, e.g. $[\text{NH}_2\text{R}_2]^+$. As the reaction is done in pivalic acid, we simply add the secondary amine which is protonated in situ, generating a template [33].

The result is remarkable; chromatographic separation is rarely, although occasionally, necessary as the $[\text{NH}_2\text{R}_2][\text{Cr}_7\text{MF}_8(\text{O}_2\text{CCMe}_3)_{16}]$ salt (Fig. 9) seems to be strongly favoured over formation of the neutral $[\text{Cr}_8\text{F}_8(\text{O}_2\text{CCMe}_3)_{16}]$. Immediately, it was obvious we could vary R—all linear alkyls from Me to n -octyl work perfectly

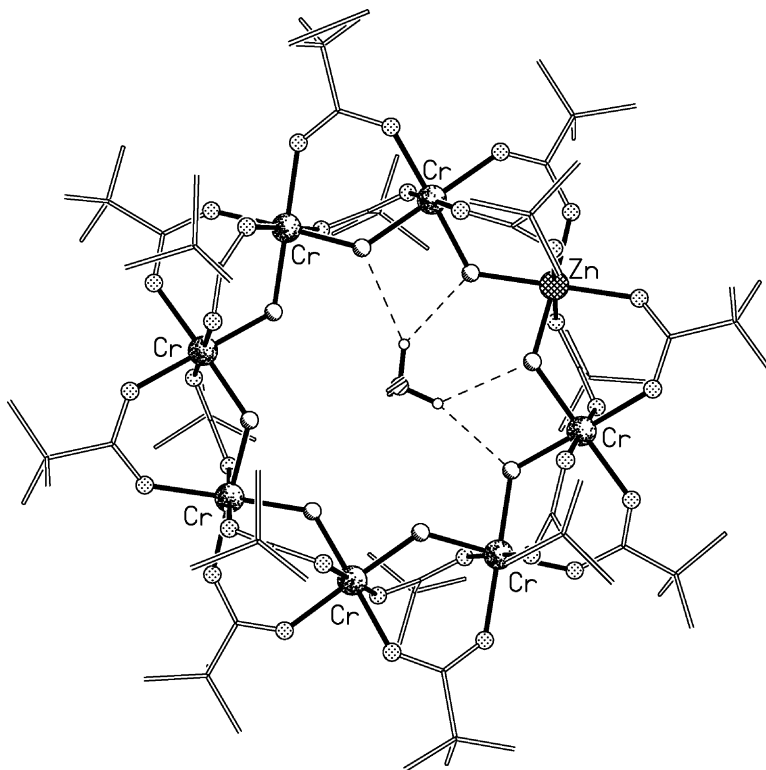


Fig. 9. The structure of a representative octanuclear heterometallic wheel: $[\text{NH}_2\text{Et}_2][\text{Cr}_7\text{ZnF}_8(\text{O}_2\text{CCMe}_3)_{16}]$ in the crystal. (Based on data in [33].)

well—and M, which can be Mn(II), Fe(II), Co(II), Ni(II), Zn(II) or Cd(II) [33]. The result is that not only can we make one heterometallic ring, we can make a family containing more than thirty members by minor changes in procedure.

This is important because by changing M, we can change the spin of the ground state. For example, if $\text{M}=\text{Ni(II)}$ the spin on the single ion is $S=1$. Therefore, in the ground state, we have four Cr centres aligned in one direction and three Cr and one Ni ion spins aligned in the opposite direction: the ground state is, therefore, given by $4 \times 3/2 - (3 \times 3/2 + 1) = 1/2$. For the other molecules $\{\text{Cr}_7\text{Cd}\}$ and $\{\text{Cr}_7\text{Zn}\}$ have $S=3/2$ ground states. $\{\text{Cr}_7\text{Fe}\}$ has an $S=1/2$ ground state but with the unpaired spin in the $\{\text{Cr}_3\text{M}\}$ sub-lattice whereas in $\{\text{Cr}_7\text{Ni}\}$ electron the additional electron is in the $\{\text{Cr}_4\}$ sub-lattice. As the Loss predictions [29] for the behaviour of these molecules depend on the value of the spin of the ground state, the fact that we can create molecules with different spins (1/2, 1 or 3/2) is valuable. The value of changing R was less immediately obvious, other than allowing us to vary the crystal packing of the $\{\text{Cr}_7\text{M}\}$ rings [33]. However, it is now apparent that this variation can be even more interesting.

Initially we have concentrated on fully characterising these rings and making preliminary studies of their possible applications in areas as varied as magnetic cooling and quantum computing. These studies have included inelastic neutron scattering studies, in collaboration with Prof Roberto Caciuffo (Ancona) [34] and specific heat measurements, in collaboration with Dr. Marco Affronte (Modena) [35]. In

Manchester, we have concentrated on EPR spectroscopy as these molecules all give rich EPR spectra. In general, at ca. 5–10 K, we see resonances for the ground state and one or more excited states. We can then use these spectra to obtain spin Hamiltonian parameters for all the observed states and then use this data to demonstrate how these parameters, which are a property of the molecular assembly, are related to the single ion parameters and to exchange interactions [36]. The range of compounds available makes this study particularly informative. For example, understanding how cluster ZFS depends on single ion terms is a vital consideration if we are ever to design better SMMs.

3.3. Possible applications of $\{\text{Cr}_7\text{M}\}$

Immediate applications investigated depend on the heterometal. For $\{\text{Cr}_7\text{Cd}\}$, we have begun collaborating with Dr. Marco Affronte (INFN Modena), looking at using the rings in magnetic cooling by exploiting the magneto-caloric effect (MCE) [35]. Specific heat measurements confirm that the ring has an $S=3/2$ ground state and can be simulated with $D/k = -0.31$ K; the $M_s = \pm 3/2$ levels are, therefore, lowest in energy and degenerate in zero-field; the degeneracy of the lowest lying states in zero-field is a requirement for MCE. The second requirement is that these states should split rapidly in applied field, and the Zeeman splitting of a pair of $M_s = \pm 3/2$ states will be $3g\mu_B H$. Therefore, in moderate fields, the magnetic entropy tends to zero at low temperatures as the system populates exclusively the lower energy M_s level. The dif-

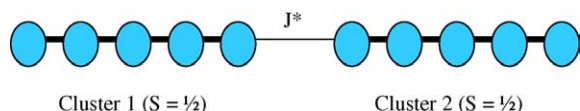


Fig. 10. A schematic representation of a proposal for a two-Qubit quantum gate.

ference in the magnetic entropy in a 7 T external field and zero-field reaches a maximum at ca. 1.5 K. The behaviour is not dissimilar to that of magnetic refrigerants used for low temperature cooling.

A “sexier” application is in quantum computing. Papers have continued to appear from the Loss group [30,31] on predictions of interesting behaviour for AF-coupled cages. Of particular interest was a pair of papers describing “two Qubit gates” based on a weakly coupled pair of $S = 1/2$ clusters. Schematically, this can be shown in Fig. 10. There are many questions about whether our AF-rings with an $S = 1/2$ ground state can be used. The first set of questions concern the parameters that determine the behaviour of individual $S = 1/2$ rings. We have, therefore, spent considerable effort characterising the $\{\text{Cr}_7\text{Ni}\}$ rings in detail. Some aspects, which chemists would take for granted, are important if a future application in “quantum information processing” is foreseen [37]. These physical quantities are:

- the extent to which the ground state can be accurately described as a two-state system, i.e. is the ground state a “pure” $S = 1/2$ state which is written as $|S, M_S\rangle$ where the two ground state is then a doublet labelled $|1/2, -1/2\rangle$ and $|1/2, +1/2\rangle$. If S contains significant admixtures of higher spin states, then the discussion is meaningless. For $\{\text{Cr}_7\text{Ni}\}$, the ground state is an $S = 1/2$ doublet, and there is very little mixing from higher S states; i.e. the state is 99% $S = 1/2$ and S is a good quantum number for discussing the lowest eigenstates of $\{\text{Cr}_7\text{Ni}\}$.
- Also important is the energy gap to the first excited state—if the gap is too small we would have to consider other values of S in describing the system. The energy difference in $\{\text{Cr}_7\text{Ni}\}$ is around 13 K, between the ground state doublet and the first excited states (an $S = 3/2$ quartet); this is sufficiently large that at low temperature the only energy levels that concern us will be $|1/2, -1/2\rangle$ and $|1/2, +1/2\rangle$. These can, therefore, be regarded as equivalent to the 0 and 1 levels of a “bit” in computation.
- Next, the $|1/2, -1/2\rangle$ and $|1/2, +1/2\rangle$ must separate in field (this is the Zeeman splitting), so that we can populate one in preference to the other without inducing significant leakage to the higher S states. This is called “initialisation” and can be imagined as creating a “bit” of information as either 0 or 1. At an external field of 2 T, the Zeeman splitting is around 2.4 K, while the energy gap to the lowest level that arises from the $S = 3/2$ quartet is still 9.4 K [37].

Unfortunately there is one more factor, and that is the loss of information to the rest of the system, which is called “de-

coherence”. Two sources of decoherence can be identified: dipolar exchange between molecules, which is easily minimised by placing the $\{\text{Cr}_7\text{Ni}\}$ rings in a matrix of diamagnetic $\{\text{Cr}_8\}$ rings. The second source is hyperfine interactions between the unpaired electron and nuclear spins. The presence of eight bridging fluorides introduces this possibility, which is not resolved by EPR spectroscopy, but which still interact sufficiently strongly with the unpaired electron as to provide a method for losing the stored information to fluctuations of the nuclear spins. As a result, decoherence rates are still too high for $\{\text{Cr}_7\text{Ni}\}$ to be useful. We believe we can remove the fluorides from the system by changing the chemical synthesis; this is the next synthetic challenge. We have already managed to make the homometallic equivalent, $[\text{Cr}(\text{OH})(\text{O}_2\text{CCMe}_3)_2]_8$ [38].

3.4. Wheels containing non-octahedral metal divalent metal ions

If the second metal present does not favour a regular octahedral geometry further new structural types are formed [39]. If the second metal ion is vanadyl, one coordination site is blocked by the oxide, thus fewer sites are available for bridging. As a result, the cage has the formula $[\text{R}_2\text{NH}_2][\text{Cr}_6(\text{VO})_2\text{F}_8(\text{O}_2\text{CCMe}_3)_{15}]$ ($\text{R} = \text{Me}, \text{Et}, n\text{-Pr}$) and contains an octanuclear core, bridged by eight fluorides as in 4 [39] (Fig. 11). The two vanadyl units are next to one another, and bridged by one pivalate in addition to a μ -fluoride, whereas all the $\text{Cr} \cdots \text{Cr}$ and $\text{Cr} \cdots \text{V}$ vectors are bridged by two pivalates and a fluoride—as in all the previous rings. The ring is a monoanion, and encapsulates a secondary ammonium cation as in the $\{\text{Cr}_7\text{M}\}$ rings. It is noticeable that the V–F bond *trans* to the oxo-group is very long (av. 2.20 Å)

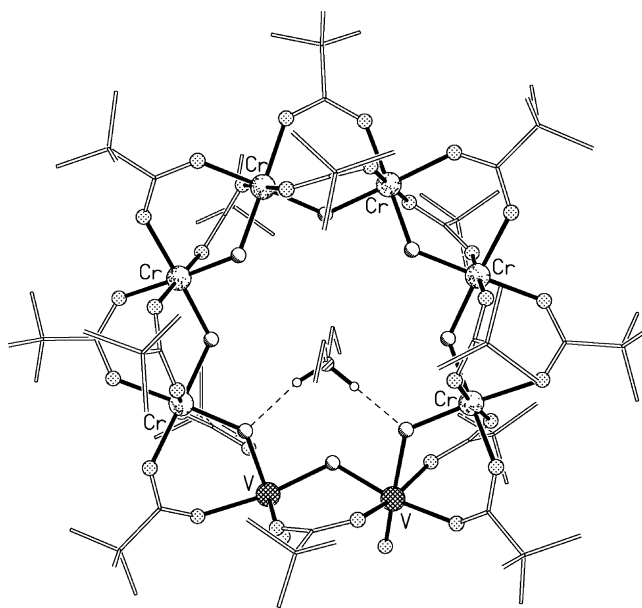


Fig. 11. The structure of $[\text{Et}_2\text{NH}_2][\text{Cr}_6(\text{VO})_2\text{F}_8(\text{O}_2\text{CCMe}_3)_{15}]$ in the crystal. (Based on data in [39].)

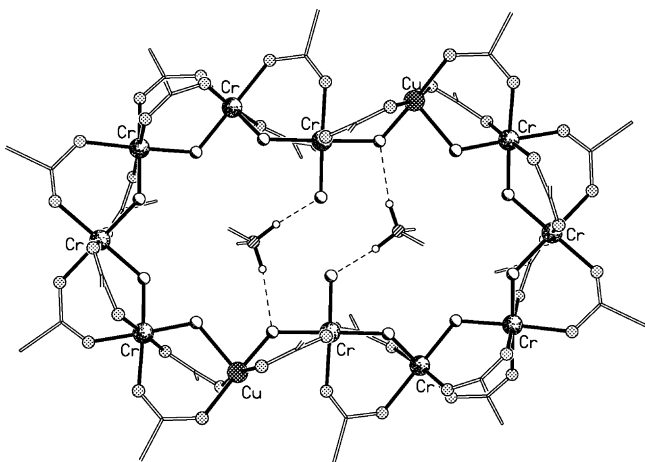


Fig. 12. The structure of $[\text{Me}_2\text{NH}_2]_2[\text{Cr}_{10}\text{Cu}_2\text{F}_{14}(\text{O}_2\text{CCMe}_3)_{22}]$ in the crystal. (Based on data in [39].)

compared to the V–F bonds *cis* to the oxo (av. 1.98 Å). The coordination geometry about V is, therefore, an extremely distorted octahedron, while the Cr^{III} ions have comparatively regular geometries.

If we use basic copper carbonate as the source of the divalent metal ion, the resulting cage is $[\text{Me}_2\text{NH}_2]_2[\text{Cr}_{10}\text{Cu}_2\text{F}_{14}(\text{O}_2\text{CCMe}_3)_{22}]$ [39], which contains a distorted dodecanuclear ring where five Cr^{III} centres lie between the two Cu^{II} centres (Fig. 12). The copper(II) centres are five-coordinate, bridged to one Cr^{III} through one fluoride and two pivalates, and to a second Cr^{III} through only one fluoride and one pivalate. A terminal fluoride is found on the neighbouring chromium. The presence of two dicationic metal ions in the ring makes the ring a dianion. Therefore, two secondary ammonium cations are found at the centre of the structure. They form H-bonds to the terminal fluorides ($\text{N} \cdots \text{F}$, 2.65 Å), and to the fluoride bridging Cu^{II} and Cr^{III} ($\text{N} \cdots \text{F}$, 3.03 Å). It is possibly the presence of H-bonds leads to a pronounced distortion of the dodecanuclear ring. In previous dodecanuclear rings, the structure is regular, e.g. in $\{\text{Ni}_{12}\}$ rings [40] the molecule has S_6 crystallographic symmetry, while in a recently reported $\{\text{Fe}_{12}\}$ ring [41] the array of metal centres has approximate six-fold symmetry. $\{\text{Cr}_{10}\text{Cu}_2\}$ is the first example of a cyclic 3d-metal complex where there are regions of negative and positive curvature: Müller et al. have stressed that growth of nanoscale polyoxomolybdates (and other nanoscale molecules) may depend on such symmetry breaking [42]. The distortion also suggests that if the two terminal fluoride bridges could be displaced by a single extended bridge it might be possible to convert **4** into a bicyclic system.

3.5. Chromium horseshoes

If only the secondary amine is added, green crystals can still be grown, however, the X-ray structural analysis of these crystals reveals formation of a new

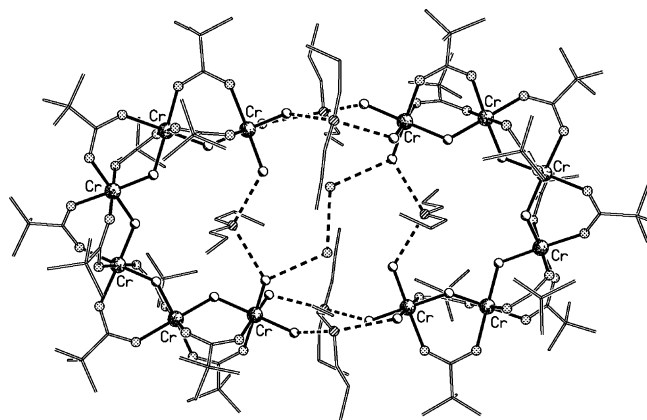


Fig. 13. The structure of $[(^n\text{Pr}_2\text{NH}_2)_3\{\text{Cr}_6\text{F}_{11}(\text{O}_2\text{CCMe}_3)_{10}\}\text{H}_2\text{O}]_2$ in the crystal. (Based on data in [39].)

structure [39]. The general formula for these new cages is $[(\text{R}_2\text{NH}_2)_3\{\text{Cr}_6\text{F}_{11}(\text{O}_2\text{CCMe}_3)_{10}\}\text{H}_2\text{O}]_2$ ($\text{R} = \text{Et}$, ^nPr , pentyl) (Fig. 13). The $[\text{Cr}_6\text{F}_{11}(\text{O}_2\text{CCMe}_3)_{10}]^{3-}$ horseshoes can be described as derived from **4** by removal of two of the Cr sites. The two Cr sites at the tips of the horseshoe have three terminal fluoride ligands. Two of these fluorides on each chromium hydrogen bond to H-atoms of $[\text{R}_2\text{NH}_2]^+$ cations, which lie between the tips of the horseshoes. These eight $\text{F} \cdots \text{H}-\text{N}$ bonds, therefore, create a dodecanuclear pseudo-macrocycle. The third fluoride on each terminal Cr site accept H-bonds from two further $[\text{R}_2\text{NH}_2]^+$ cations which are encapsulated within the pseudo-macrocycle.

Two water molecules are encapsulated within the pseudo-macrocycle, H-bonding to two fluorides, one derived from each horseshoe. The result is a supramolecule consisting of two hexametallate trianions, six ammonium cations and two water molecules. These horseshoes have an $S = 0$ ground state [39].

3.6. Other templates

As secondary amines containing linear alkyl chains give octametallate rings it was obvious to examine what happens with larger ammonium templates [43]. If we use secondary amines but with branched alkyl chains ($\text{R} = \textit{iso}$ -propyl or cyclohexyl) we generate nonanuclear wheels: $[\text{NH}_2\text{R}_2][\text{Cr}_8\text{MF}_9(\text{O}_2\text{CCMe}_3)_{18}]$ ($\text{M} = \text{Ni}$, Co or Cd thus far) (Fig. 14). These are the first large odd-numbered rings containing paramagnetic ions. Odd-numbered rings are rare in general; other than the oxo-centred triangles, e.g. [4] there are only three reports of pentanuclear rings—a metallocrown made by the Pecararo group [44], an $\{\text{Fe}_5\}$ ring made by the Lehn group [45] (which graced the cover of *Angew. Chem.*), and a pentagon made by Dunbar and co-workers [46].

These rings are, therefore, worth investigating. $\{\text{Cr}_8\text{Co}\}$ is initially disappointing—showing behaviour similar to $\{\text{Cr}_7\text{Co}\}$ —but $\{\text{Cr}_8\text{Ni}\}$ is exciting [43]. A plot of χ against T shows two maxima—which is unprecedented for a “simple” paramagnetic ring. The ground state appears to be $S = 0$,

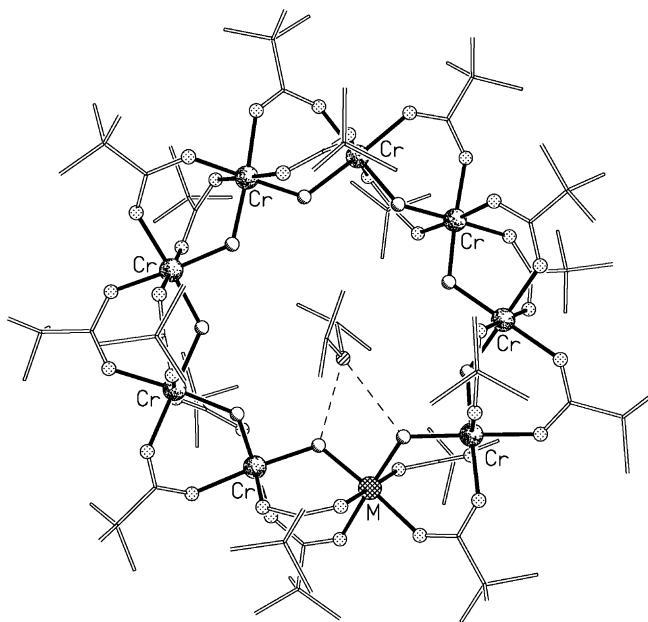


Fig. 14. The structure of $[\text{NH}_2^i\text{Pr}_2][\text{Cr}_8\text{MF}_9(\text{O}_2\text{CCMe}_3)_{18}]$ in the crystal ($\text{M} = \text{Ni}$ or Co). (Based on data in [43].)

which implies that the spins on the metal sites cannot be treated as “classical” spins. A detailed analysis—performed by Olivier Cador and Roberta Sessoli—shows that the double maxima reflects the presence of low-lying $S = 1$ excited states near the $S = 0$ ground state, and that a spin ladder containing such low-lying states arises if the Cr–Ni exchange interaction is around 30 cm^{-1} , cf. a Cr–Cr exchange of 10 cm^{-1} [43].

While the system is not spin frustrated if a narrow definition of frustration is adopted [47]—the molecule has an even number of electrons, therefore, can reach a non-degenerate $S = 0$ ground state—it is certainly impossible in an anti-ferromagnetically coupled nonanuclear ring for the spins to alternate “up and down” as a simple-minded picture of an AF-ring would require. The picture we have adopted describes $\{\text{Cr}_8\text{Ni}\}$ as a “magnetic Möbius strip” [43]. The AF-structure—alternate spin up and down—is fairly regular near the Ni(II) site, as the Cr–Ni exchange is larger, but on the Cr-chain, the structure becomes irregular as it is impossible for all the spins to be anti-parallel to those on their nearest neighbours. The one-edged, one-face Möbius strip is a good metaphor for this structure, with the “twist” in the strip being equivalent to the point in the magnetic structure where the AF-structure is least regular.

If we go further, and use a tertiary amine, e.g. dicyclohexylethylamine, we generate decametallic rings, e.g. $[\text{Cr}_9\text{NiF}_{12}(\text{O}_2\text{CCMe}_3)_{18}]^-$ [48]. The ring is not as regular as the octa- and nona-metallic rings as two $\text{M} \cdots \text{M}$ edges are bridged by two fluorides and a carboxylate, unlike the usual one fluoride and two carboxylates. We are beginning to look at still larger amine templates hoping to make the first undecametallic rings.

More imaginatively, and much less rationally, we thought it worth examining more complex amines [49]. As sam-

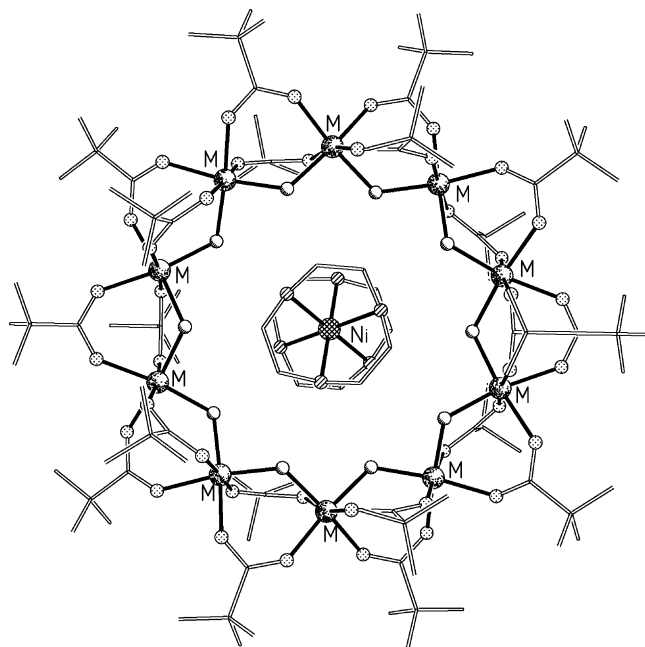


Fig. 15. The structure of $[\text{Ni}(9\text{-ane-N}_3)_2][\text{Cr}_8\text{Ni}_2\text{F}_{10}(\text{O}_2\text{CCMe}_3)_{20}]$ in the crystal. The eight Cr and two Ni sites in the decanuclear wheel are disordered (labelled M). (Based on data in [49].)

ples of both 9-ane- N_3 and 12-ane- N_4 (where 9-ane- N_3 is 1,4,7-triazacyclononane [tacn] and 12-ane- N_4 is 1,4,7,10-tetraazacyclododecane [cyclen]) were available in the laboratory we used those as templates for formation of rings. In both cases, the result is unexpected, and extremely beautiful. Thus, reaction of $\text{CrF}_3 \cdot 4\text{H}_2\text{O}$, basic nickel carbonate and pivalic acid in the presence of the macrocycle leads first to complexation of Ni(II) by the macrocycle, and the metal–macrocycle complex then acts as the “template” for the remainder of the structure. The chemistry works better if the Ni macrocycle complex is pre-formed before addition to the reaction mixture.

With 9-ane- N_4 , we make a new decametallic ring, templated about a $[\text{Ni}(9\text{-ane-N}_3)_2]^{2+}$ complex: $[\text{Ni}(9\text{-ane-N}_3)_2][\text{Cr}_8\text{Ni}_2\text{F}_{10}(\text{O}_2\text{CCMe}_3)_{20}]$ [49] (Fig. 15). The decametallic ring is a regular decagon and the central complex is only weakly H-bonded to the exterior ring. The magnetic behaviour tells us a good deal about how the complex forms. The low temperature value for the susceptibility is consistent with an $S = 1$ ground state, i.e. the susceptibility is due to the central $[\text{Ni}(9\text{-ane-N}_3)_2]$ divalent cation; the spins in the decametallic ring must cancel, giving an $S = 0$ ground state. For this to happen there have to be two $\{\text{Cr}_4\text{Ni}\}$ sub-lattices to balance the spins and reach $S = 0$. This happens most naturally if alternate sites are “spin up” with the others “spin down”. If we consider the odd-numbered sites as “spin up”, and the even sites as “spin down”, this means that one nickel must be on an odd site and the other on an even site. There are three possibilities: the Ni sites could be neighbours, in 1,2 positions of the 10-membered metal ring, separated by two Cr ions (at 1,4-positions) or separated by four Cr ions (at 1,6-positions).

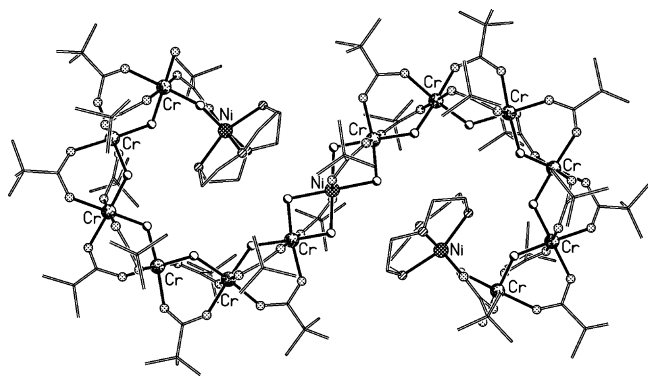


Fig. 16. The structure of $[\text{Ni}(\text{cyclen})]_2\text{Cr}_{12}\text{NiF}_{18}(\text{O}_2\text{CCMe}_3)_{24}$ in the crystal. (Based on data in [49].)

While the latter two are possibilities, the first option—that the Ni sites are neighbours—seems much the most probable. This, in turn, suggests that the cluster forms from an open chromium chain, and the final cyclic product is formed when the heterometal ion is attached. We have further—equally circumstantial—evidence for this proposition (see below).

If we use 12-ane- N_4 , the resulting structure is even more beautiful [49]. $[\text{Ni}(\text{cyclen})]_2\text{Cr}_{12}\text{NiF}_{18}(\text{O}_2\text{CCMe}_3)_{24}$ is a wholly unexpected product, but is related to previous the $\{\text{Cr}_6\}$ horseshoes discussed above. The 15 metal sites describe an “S”, with a Ni^{II} ion at the centre of the “S”, and the two Ni^{II} ions within [12]-ane- N_4 rings at the termini of the “S” (Fig. 16). The cyclen macrocycles bind in the usual manner, leaving *cis*-vacancies on the coordinated Ni^{II} , and it is the two atoms occupying these *cis*-sites that link the $\{\text{Ni}([12]\text{-ane-N}_4)\}^{2+}$ fragment to the termini of the metal chain. The 12 Cr^{III} ions form two hexametallc chains, with these chains being very similar to the anionic $\{\text{Cr}_6\}$ horseshoes discussed above. The metal core is almost planar with the mean deviation from planarity being 0.25 Å. Magnetic studies of the molecular “S” or “seahorse” show it has an $S = 1$ ground state [49].

3.7. Some thoughts on how the heterometallic wheels form

The heterometallic wheels have a rather simple composition with the metal ions bonded by two bridging ligands. Compared with most polymetallic clusters the presence of only two ligands is restrained [32]. One ligand is a carboxylate, a common ligand for a large number of polynuclear metal complexes, which normally also contain oxo-, hydroxo- and/or alkoxo- bridges. The second ligand is fluoride. Single fluoride bridges are quite common in dimers, but polymetallic cages featuring fluoride are quite rare [50–52].

Three key features of fluorine/fluoride favour formation of these structures. Firstly, it is clear from the structures above that the M-F-M angle is very flexible, with these angles varying from 60 to 180°. Secondly, fluorine is the most elec-

tronegative element and forms very strong bonds to most other elements. The strength of the Cr-F bond here is probably a necessary factor in the formation of these structures. The third factor is the small size of the F^- ion, which does not restrict formation of these cyclic structures.

Formation of the structures is an intriguing question. Isolation of the chromium horseshoes has allowed us to perform three experiments that suggest that “chromium horseshoes”, or more generally *acyclic* chromium-fluoride chains are intermediate products in the “metallomacrocyclization” reaction.

The experiments were:

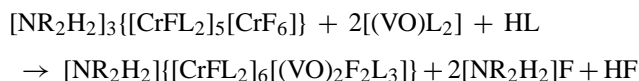
- (b) To a solution of $[\text{Cr}_8\text{F}_8(\text{O}_2\text{CCMe}_3)_{16}]$ in pivalic acid was added a source of a second metal dication $[\text{Ni}_2(\text{H}_2\text{O})(\text{O}_2\text{CCMe}_3)_4(\text{HO}_2\text{CCMe}_3)_4]$ [53] and *n*-dipropylamine. The mixture was heated at the same time and temperature as required for the synthesis of heterometallic $\{\text{Cr}_7\text{M}\}$ wheels. Very little $[(^n\text{Pr})_2\text{NH}_2][\text{Cr}_7\text{NiF}_8(\text{O}_2\text{CCMe}_3)_{16}]$ was detected by mass spectrometry on analysis of this reaction; the vast majority of the compounds remains unreacted.
- (c) To a solution of a “double horseshoe”, $[(\text{R}_2\text{NH}_2)_3\{\text{Cr}_6\text{F}_{11}(\text{O}_2\text{CCMe}_3)_{10}\}]_2$ ($\text{R} = \text{Et}$ or ^nPr) in pivalic acid was added only $[\text{Ni}_2(\text{H}_2\text{O})(\text{O}_2\text{CCMe}_3)_4(\text{HO}_2\text{CCMe}_3)_4]$ and the mixture was left to react as in previous experiment. $\{[\text{R}_2\text{NH}_2][\text{Cr}_7\text{NiF}_8(\text{O}_2\text{CCMe}_3)_{16}]\}$ was formed quantitatively for both amines.
- (d) Simple recrystallisation at room temperature of the “double horseshoes” from formic acid leads to replacement of terminal fluorides from the structure without changing the bridging within the chromium chain [54].

Experiment (a) suggests that $[\text{Cr}_8\text{F}_8(\text{O}_2\text{CCMe}_3)_{16}]$ is kinetically stable with respect to ligand displacement and, as chromium(III) is unreactive, it is very difficult to replace one $\text{Cr}(\text{III})$ to one $\text{Ni}(\text{II})$ ion once the homometallic octanuclear ring has formed. Experiment (b) suggests that the horseshoe can be very readily converted into the heterometallic ring. Experiment (c) implies that the bridging fluorides are less reactive than the terminal fluorides in the horseshoes, i.e. the two M-F bonds make the F^- ions unreactive as well as the $\text{Cr}(\text{III})$.

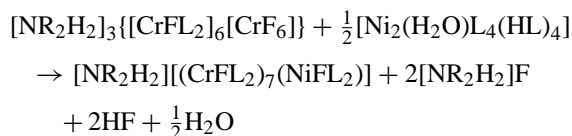
The individual horseshoes can be recognised as fragments of the heterometallic wheels, but with many additional extra terminally fluoride anions: we could write a general formula for the homometallic chains and wheels as $[\text{CrFL}_2]_n[\text{CrF}_6^{3-}]_m$ (where $n = 8$, $m = 0$ for wheels, and $n = 5$, $m = 1$ for chains). The additional negative charge in the open-chains is compensated by protonated amines, with two amines at each end of the horseshoes and an additional protonated amine at the centre of each horseshoe. As long as the protonated amine in the centre of horseshoe remains, we can envisage displacing the remaining two protonated amines by metal dication. As the yields of heterometallic wheels are remarkably high for polynuclear complexes, it is reasonable to write stoichiometric equations for the transformations. The

formulae have been re-written to stress the CrFL_2 repeat units present in all these structures.

The simplest case here is the formation of $[\text{NR}_2\text{H}_2][\text{Cr}_6(\text{VO})_2\text{F}_8\text{L}_{15}]$ (L =pivalate) which we could write as:

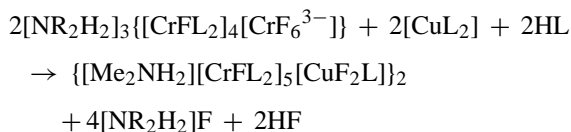


This reaction can be easily justified as the length of the acyclic chromium(III) chain is the same as the number of chromium centres in the resulting heterometallic wheel. For the $\{\text{Cr}_7\text{M}\}$ wheels, the reaction (for $\text{M}=\text{Ni}$) is:



The cages can also be formed by addition of metal carbonates to the solution in pivalic acid, which presumably generates M complexes of L in situ. The equation balances best if the acyclic chain contains seven $\text{Cr}(\text{III})$ centres, not six.

For $\{\text{Cr}_{10}\text{Cu}_2\}$, a stoichiometric equation can be written, but starting with a pentanuclear $\text{Cr}(\text{III})$ chain:



The heterometallic rings, therefore, can be regarded as completing acyclic chromium chains that can be penta-, hexa- or hepta-nuclear. This idea has made us look for the other chains; by using *iso*-propylamine we have succeeded in isolating $[(^i\text{Pr}_2\text{NH}_2)_3\{\text{Cr}_7\text{F}_{12}(\text{O}_2\text{CCMe}_3)_{12}\}]_2$ [55], which at least suggests the concept is feasible.

The protonated amine cations, therefore, have two distinct roles in the formation of the heterometallic rings. Firstly, the protonated amines bind to the acyclic chains, preventing the formation of the cyclic $[\text{Cr}_8\text{F}_8(\text{O}_2\text{CCMe}_3)_{16}]$ molecule—which is unreactive. As long as the ring remains open, interchange between various $[\text{CrFL}_2]_n[\text{CrF}_6^{3-}]$ chains is possible because the terminal fluorides and their associated protonated amines can exchange. These “terminal” protonated amines can be lost or gained, allowing an equilibrium to be established between the chromium chains present. The central protonated amine, which forms many more H-bonds to the “horseshoe”, is not as easily displaced. Addition of the second metal dication allows a cyclic (and hence unreactive) structure to form, without loss of the strongly bound protonated amine template. Curiously, while the neutral $\{\text{Cr}_8\}$ wheel has a negative electrostatic potential for the host cavity due to the presence of the fluoride bridges, it does not bind to ammonium cations [56]. Therefore, cyclisation to the homometallic ring would require loss of this central ammo-

nium. Probably, it is more thermodynamically convenient for the system to accept a compatible bivalent metal cation in the ring than to remove the cation accommodated in the host cavity of the wheel.

Such mechanisms are difficult to prove, but they suggest intriguing new reactions using “horseshoes” for directed synthesis. If the stoichiometric reactions given above are correct, or even approximately accurate, reaction of the horseshoes with heterometallic carboxylate complexes should be possible. So, for example, it should be possible to make $[(\text{C}_3\text{H}_7)_2\text{NH}_2][\text{Cr}_6\text{FeNiF}_8(\text{O}_2\text{CCMe}_3)_{16}]$ from the simple reaction of $[(\text{R}_2\text{NH}_2)_3\{\text{Cr}_6\text{F}_{11}(\text{O}_2\text{CCMe}_3)_{10}\}\text{H}_2\text{O}]_2$ ($\text{R}=\text{Pr}$) with $[\text{Fe}_2\text{NiO}(\text{O}_2\text{CCMe}_3)(\text{HO}_2\text{CCMe}_3)_3]$ [5]. This approach should lead to heterotrimetallic octa-, nona- and deca-nuclear wheels in the future.

Acknowledgments

This work has been performed with a huge number of international collaborators all of whom have made important contributions to these studies. Much of our original interest arose from conversations involving Florian Meier (Basel) and Joris van Slageren (then Firenze but now Stuttgart); endless discussions with David Collison (Manchester) have also contributed enormously. Some of the chromium cages were made by Mark Murrie and Andrew A. Smith. X-ray structures have been done by Finn Larsen and Jacob Overgaard (Aarhus, Denmark), Chris Muryn and Sarah Heath (Manchester), Simon Parsons (Edinburgh) and the many structures which required synchrotron radiation involved Simon Teat (CCLRC Daresbury). The neutron diffraction study of **1** was a collaboration with Chick Wilson (Glasgow). Magnetic measurements involved Eva Rentschler (MPI Mülheim), Oliver Cador, Roberta Sessoli and Dante Gatteschi (Firenze), Marshall Luban and Paul Kögerler (Ames Lab, Iowa). Single crystal measurements have been performed with Wolfgang Wernsdorfer (Grenoble). Inelastic neutron scattering studies have involved Roberto Caciuffo and Tatiana Guidi (Ancona). Specific heat measurements have been done with Marco Affronte (INFN Modena) and his colleagues. Predictions concerning uses in quantum computing arise from the group of Stefano Carreta (Parma). Optical measurements were done with Andrew Thomson (UEA). Studies of hybrid materials were done by Clement Sanchez (Paris-VI), Talal Mallah and Guillaume Rogez (Paris-Sud). Funds spent in Manchester came from the EPSRC (UK), the EC-RTNs “MolNanoMag” and “QueMolNa”, the Royal Society, INTAS and the University of Manchester.

References

- [1] S.M. Gorun, G.C. Papaefthymiou, R.B. Frankel, S.J. Lippard, *J. Am. Chem. Soc.* 109 (1987) 3337.
- [2] G. Aromi, S.M.J. Aubin, M.A. Bolcar, G. Christou, H.J. Eppley, K. Folting, D.N. Hendrickson, J.C. Huffman, R.C. Squire, H.-L. Tsai, S. Wang, M.W. Wemple, *Polyhedron* 17 (1998) 3005.

- [3] A. Caneschi, D. Gatteschi, R. Sessoli, P. Rey, *Acc. Chem. Res.* 22 (1989) 392.
- [4] I. Mulyani, A. Levina, P. Lay, *Angew. Chem. Int. Ed.* 43 (2004) 4504.
- [5] R.D. Cannon, R.P. White, *Prog. Inorg. Chem.* 36 (1988) 195.
- [6] A.S. Batsanov, G.A. Timco, N.V. Struchkov, N.V. G rb    , K.M. Indrichan, *Koord. Khim.* 17 (1991) 662.
- [7] N.V. Gerbelev, Yu.T. Struchkov, G.A. Timco, A.S. Batsanov, K.M. Indrichan, G.A. Popovich, *Dokl. Akad. Nauk. SSSR* 313 (1990) 1459.
- [8] F.E. Mabbs, E.J.L. McInnes, M. Murrie, S. Parsons, G.M. Smith, C.C. Wilson, R.E.P. Winpenny, *Chem. Commun.* (1999) 643.
- [9] D. Collison, M. Murrie, V.S. Oganessian, S. Piligkos, N.R.J. Poolton, G. Rajaraman, G.M. Smith, A.J. Thomson, G.A. Timco, W. Wernsdorfer, R.E.P. Winpenny, E.J.L. McInnes, *Inorg. Chem.* 42 (2003) 5293.
- [10] S. Piligkos, D. Collison, V.S. Oganessian, G. Rajaraman, G.A. Timco, A.J. Thomson, R.E.P. Winpenny, E.J.L. McInnes, *Phys. Rev. B* 69 (2004) 134424/1.
- [11] M.N. Leuenberger, D. Loss, *Nature* 410 (2001) 789.
- [12] S. Piligkos, D. Collison, V.S. Oganessian, A.J. Thomson, G.A. Timco, R.E.P. Winpenny, E.J.L. McInnes, *J. Am. Chem. Soc.* 125 (2003) 1168.
- [13] S. Sugano, M. Peter, *Phys. Rev.* 122 (1961) 381.
- [14] B.R. McGarvey, *J. Chem. Phys.* 41 (1964) 3743.
- [15] R.M. Macfarlane, *J. Chem. Phys.* 39 (1963) 3118.
- [16] R.M. Macfarlane, *J. Chem. Phys.* 47 (1967) 2066.
- [17] A. Bencini, D. Gatteschi, *EPR of Exchange Coupled Systems*, Springer-Verlag, Berlin, 1989.
- [18] I.M. Atkinson, C. Benelli, M. Murrie, S. Parsons, R.E.P. Winpenny, *Chem. Commun.* (1999) 285.
- [19] M. Luban, P. Kogerler, L.L. Miller, R.E.P. Winpenny, *J. Appl. Phys.* 93 (2003) 7083.
- [20] S. Parsons, A.A. Smith, R.E.P. Winpenny, *Chem. Commun.* (2000) 579.
- [21] M. Eshel, A. Bino, *Inorg. Chim. Acta* 329 (2002) 45.
- [22] T. Coradin, T. Mallah, G. Rogez, C. Sanchez, A.A. Smith, R.E.P. Winpenny, *Adv. Mater.* 14 (2002) 896.
- [23] N.V. Gerbelev, A.S. Batsanov, G.A. Timco, Yu.T. Struchkov, K.M. Indrichan, G.A. Popovich, *Patent SU No. 1299116*, Priority date 1985-08-07.
- [24] J. van Slageren, R. Sessoli, D. Gatteschi, A.A. Smith, M. Hellwell, R.E.P. Winpenny, A. Cornia, A.-L. Barra, A.G.M. Jansen, G.A. Timco, E. Rentschler, *Chem. Eur. J.* 8 (2002) 277.
- [25] K.L. Taft, C.D. Delfs, G.C. Papaefthymiou, S. Foner, D. Gatteschi, S.J. Lippard, *J. Am. Chem. Soc.* 116 (1994) 823.
- [26] S. Carretta, J. van Slageren, T. Guidi, E. Livioiti, C. Mondelli, D. Rovai, A. Cornia, A.L. Dearden, F. Carsughi, M. Affronte, C.D. Frost, R.E.P. Winpenny, D. Gatteschi, G. Amoretti, R. Caciuffo, *Phys. Rev. B* 67 (2003) 094405/1.
- [27] O. Waldmann, T. Guidi, S. Carretta, C. Mondelli, A. Dearden, *Phys. Rev. Lett.* 91 (2003) 237202/1.
- [28] O. Waldmann, *Coord. Chem. Rev.* 249 (2005) 2550.
- [29] F. Meier, D. Loss, *Phys. Rev. B* 64 (2001) 224411/1.
- [30] F. Meier, J. Levy, D. Loss, *Phys. Rev. Lett.* 90 (2003) 047901.
- [31] F. Meier, J. Levy, D. Loss, *Phys. Rev. B* 68 (2003) 134417.
- [32] R.E.P. Winpenny, in: J.A. McCleverty, T.J. Meyer (Eds.), *Comp. Coord. Chem. II* 7 (2004) 125.
- [33] F.K. Larsen, E.J.L. McInnes, H. El Mkami, J. Overgaard, S. Piligkos, G. Rajaraman, E. Rentschler, A.A. Smith, G.M. Smith, V. Boote, M. Jennings, G.A. Timco, R.E.P. Winpenny, *Angew. Chem. Int. Ed.* 42 (2003) 101.
- [34] R. Caciuffo, T. Guidi, G. Amoretti, S. Carretta, E. Livioiti, P. Santini, C. Mondelli, G. Timco, C.A. Muryn, R.E.P. Winpenny, *Phys. Rev. B*, accepted for publication.
- [35] M. Affronte, A. Ghirri, S. Carretta, G. Amoretti, S. Piligkos, G.A. Timco, R.E.P. Winpenny, *Appl. Phys. Lett.* 84 (2004) 3468.
- [36] S. Piligkos, D. Collison, E.J.L. McInnes, G.A. Timco, R.E.P. Winpenny, *J. Am. Chem. Soc.*, in preparation.
- [37] F. Troiani, A. Ghirri, M. Affronte, S. Carretta, P. Santini, G. Amoretti, S. Piligkos, G. Timco, R.E.P. Winpenny, *Phys. Rev. Lett.*, submitted for publication.
- [38] P. Christian, G. Rajaraman, A. Harrison, J.J.W. McDouall, J.T. Raftery, R.E.P. Winpenny, *Dalton Trans.* (2004) 1511.
- [39] F.K. Larsen, J. Overgaard, S. Parsons, E. Rentschler, G.A. Timco, A.A. Smith, R.E.P. Winpenny, *Angew. Chem. Int. Ed.* 42 (2003) 5978.
- [40] H. Andres, R. Basler, A.J. Blake, E.K. Brechin, C. Cadiou, G. Chaboussant, C.M. Grant, H.-U. G    , S.G. Harris, M. Murrie, S. Parsons, C. Paulsen, F. Semadini, V. Villar, W. Wernsdorfer, R.E.P. Winpenny, *Chem. Eur. J.* 8 (2002) 4867.
- [41] C.P. Raptopoulou, V. Tangoulis, E. Devlin, *Angew. Chem. Int. Ed.* 41 (2002) 2386.
- [42] A. M    , E. Beckmann, H. B    , M. Schmidtman, A. Dress, *Angew. Chem. Int. Ed.* 41 (2002) 1162.
- [43] O. Cador, D. Gatteschi, R. Sessoli, F.K. Larsen, J. Overgaard, A.-L. Barra, S.J. Teat, G.A. Timco, R.E.P. Winpenny, *Angew. Chem.* 43 (2004) 5196.
- [44] V.L. Pecoraro, A.J. Stemmler, B.R. Gibney, J.J. Bodwin, H. Wang, J.W. Kampf, A. Barwinski, *Prog. Inorg. Chem.* 45 (1997) 83.
- [45] B. Hasenknopf, J.-M. Lehn, B.O. Kneisel, G. Baum, D. Fenske, *Angew. Chem. Int. Ed.* 35 (1996) 1838.
- [46] C.S. Campos-Fern    , R. Cl    , J.M. Koomen, D.H. Russell, K.R. Dunbar, *J. Am. Chem. Soc.* 123 (2001) 773.
- [47] G. Toulouse, *Commun. Phys.* 2 (1977) 115.
- [48] G.A. Timco, C.A. Muryn, A.S. Batsanov, F.K. Larsen, J. Overgaard, R.E.P. Winpenny, unpublished results.
- [49] S.L. Heath, R.H. Laye, C.A. Muryn, R. Sessoli, R. Shaw, S.J. Teat, G.A. Timco, R.E.P. Winpenny, *Angew. Chem.* 43 (2004) 6132.
- [50] A. Bino, M. Ardon, D. Lee, B. Spingler, S.J. Lippard, *J. Am. Chem. Soc.* 124 (2002) 4578.
- [51] L.F. Jones, E.K. Brechin, D. Collison, A. Harrison, S.J. Teat, W. Wernsdorfer, *Chem. Commun.* (2002) 2974.
- [52] L.F. Jones, E.K. Brechin, D. Collison, J. Raftery, S.J. Teat, *Inorg. Chem.* 42 (2003) 6971.
- [53] G. Chaboussant, R. Basler, H.-U. G    , S. Ochsenbein, A. Parkin, S. Parsons, G. Rajaraman, A. Sieber, A.A. Smith, G.A. Timco, R.E.P. Winpenny, *Dalton* (2004) 2757.
- [54] G.A. Timco, F.K. Larsen, J. Overgaard, unpublished results.
- [55] G.A. Timco, C.A. Muryn, R.E.P. Winpenny, unpublished results.
- [56] J. Overgaard, B.B. Iversen, S.P. Pali  , G.A. Timco, N.V. Gerbelev, F.K. Larsen, *Chem. Eur. J.* 8 (2002) 2775.